

# Photowritable Silver-Containing Phosphate Glass Ribbon Fibers

Sylvain Danto, Frédéric Désévédavy, Yannick Petit, Jean-Charles Desmoulin, Alain Abou Khalil, Clément Strutynski, Marc Dussauze, Frédéric Smektala, Thierry Cardinal, Lionel Canioni

▶ **To cite this version:**

Sylvain Danto, Frédéric Désévédavy, Yannick Petit, Jean-Charles Desmoulin, Alain Abou Khalil, et al.. Photowritable Silver-Containing Phosphate Glass Ribbon Fibers. Advanced Optical Materials, 2016, 4 (1), pp.162-168. 10.1002/adom.201500459 . hal-01270527

**HAL Id: hal-01270527**
**https://hal.science/hal-01270527**

Submitted on 15 Jan 2021

**HAL** is a multi-disciplinary open access archive for the deposit and dissemination of scientific research documents, whether they are published or not. The documents may come from teaching and research institutions in France or abroad, or from public or private research centers.

L'archive ouverte pluridisciplinaire **HAL**, est destinée au dépôt et à la diffusion de documents scientifiques de niveau recherche, publiés ou non, émanant des établissements d'enseignement et de recherche français ou étrangers, des laboratoires publics ou privés.

DOI: 10.1002/((please add manuscript number))

**Article type: Full paper**

# Photo-writable Silver-containing Phosphate Glass Ribbon Fibers

*S. Danto, F. Désévédavy, Y. Petit, J-C. Desmoulin, A. Abou Khalil, C. Strutynski, M. Dussauze, F. Smektala, T. Cardinal, L. Canioni*

Dr. S. Danto, Prof. Y. Petit, J-C. Desmoulin, Dr. T. Cardinal

Institute of Chemistry of the Condensed Matter of Bordeaux (ICMCB)

University of Bordeaux

33608 Pessac – France

E-mail: sylvain.danto@u-bordeaux.fr

Dr. F. Désévédavy, C. Strutynski, Prof. F. Smektala

Laboratoire Interdisciplinaire Carnot de Bourgogne, UMR 6303 CNRS

University of Bourgogne Franche-Comté

9 Avenue Alain Savary, BP 47870 - 21078 Dijon, France

Prof. Y. Petit, Prof. L. Canioni, A. Abou Khalil

Center for Intense Lasers and Applications (CELIA)

University of Bordeaux

33405 Talence – France

Dr. M. Dussauze

Institute of Molecular Science

University of Bordeaux

33405 Talence – France

***Abstract***

Tailored silver-containing zinc-phosphate glasses possess excellent thermo-viscous ability and optical properties. Beyond they have proven to form a favorable matrix for the direct Laser writing of photo-luminescent and nonlinear patterns. Here, bringing together the merits of these materials with fiber optic technology, we report on the first photosensitive, photo-writable silver-containing glass ribbon fibers. These novel devices are thermally scaled-down in a homothetic fashion from a macroscopic preform to produce tens-of-meters of continuous structure. We demonstrate that luminescence properties of the native glass are preserved after the shaping process. Furthermore we establish that the unique fiber's flat geometry allows for the convenient, accurate Laser writing of complex luminescent silver clusters patterns within the glass matrix. We believe the drawing of silver-containing zinc-phosphate glasses could lead to a decisive breakthrough in the field of photosensitive fibers. They would offer a promising platform for the design of highly efficient sensing devices based on amplified optical processes effects, for metamaterials or as fundamental bricks for photonics.

**Keywords:** phosphate, glasses, fiber, photosensitivity, laser inscription

## 1. Introduction

Photosensitive fibers represent a ubiquitous platform for Fiber Bragg gratings (FBGs). Their discovery paved the way for the development of a multitude of *in-fiber* optical components (wavelength-selective reflectors, gain-flattening filters, chirped FBGs for pulse compression and dispersion compensation, interferometers…) ultimately forming the backbone for long-haul modern telecommunication systems or for fiber-based sensors.[1] When it comes to industrial applications, silica glass vastly dominates the field of photosensitive fibers. Tuning of their photosensitivity usually relies either on pre-drawing co-doping (intrinsic photosensitivity), or on post-drawing hydrogen-loading (extrinsic photosensitivity).[1] Beside silica, other materials may be employed for the fabrication of photosensitive fibers, including polymers, fluorides or chalcogenides glasses.[2-4] Polymers find applications too in fluorescent optical fibers for high-energy particles detection, imaging, and sensors.[5-7]

Phosphate glasses however inherently lack photosensitivity, therefore strongly limiting their amenability for Bragg's mirrors inscription into fibers. Various photo-sensitization approaches have been developed, such as ion-exchange,[8] Germanium doping[9] or UV inscription combined with photo-thermal annealing;[10] yet critical limitations (technical complexity, sensitivity, scattering loss) persist to date. Best results were obtained with the use of IR-femtosecond laser pulses and phase-masks, enabling for FBGs inscription into rare earth doped phosphate glass fibers.[11, 12]

Here we report on a novel strategy for developing intrinsically photosensitive fibers, a strategy that relies on the direct drawing of tailored silver-containing zinc-phosphate glass materials. Zinc-phosphate glasses possess good thermo-chemical durability, excellent linear optical properties and form a competing matrix for the heavy loading of homogeneously-dispersed silver ions.[13-15] Besides their interaction with a high-repetition-rate femtosecond laser yields the

formation of locally distributed silver clusters with fluorescence and 2nd-order nonlinear optical properties. While extensively studied in bulk form, attempts for the fabrication of luminescent silver-containing fibers glass remain scarce to date,[16] including to our knowledge no report on the use of phosphate glasses.

Then, going a step further in the shaping of silver-containing phosphate glasses, we introduce an innovative approach for the design of flat-substrate, sharp corner-edges fibers. Due to surface energy minimization, fiber optics' geometry has long remained narrowed down to cylindrical shapes. Yet approaches have emerged recently to overcome this limitation, which involve the drawing of stacked polymers sheets[17, 18] or of hollow silica preforms, subsequently flattened under vacuum.[19] Our method consists in the direct, homothetic shaping of a rectangular phosphate glass preform into tens-of-meters-long ribbon fibers. Key to this breakthrough is the precise control of the viscosity-regime applied to the glass during the drawing. Building on this result, we show that ribbon fibers represent a powerful platform for the Direct Laser Writing (DLW) of silver clusters motifs with elaborated profiles within the glass matrix.

The manufacturing of intrinsically photosensitive silver-containing zinc-phosphate ribbon fibers offers several important features as fully described below. To efficiently treat our research endeavor we selected the most suitable materials for the targeted application, developed the fiberization technique and adopted innovative geometry. Raman spectroscopy, together with absorption and fluorescence spectroscopies were appropriately exploited to establish the correlation between the properties of native glass composition and the fiber properties.

## 2. Results and discussion

### 2.1. Cylindrical silver-containing zinc-phosphate glass fibers

The selected tailored glass compositions with their glass transition temperatures ($T_g$), density and refractive index are specified in **Table 1**. It consists of the glasses $40P_2O_5$-55ZnO-$1Ga_2O_3$-$4Na_2O$ (hereafter PZG-4N) and $40P_2O_5$-55ZnO-$1Ga_2O_3$-$2Na_2O$-$2Ag_2O$ (hereafter PZG-2N2A). The substitution of $Na_2O$ with $Ag_2O$ (2% mol) aims to demonstrate the effect of the drawing on the luminescence properties of the glass. The materials were fabricated using a standard melt-quench technique in a platinum crucible (see *Experimental* section).

**Table 1** *Investigated glasses and related properties*

| **Glass** | **Composition (mol%)** | | | $T_g$ [±2 °C] | $\rho$ [±0.01 g.cm$^{-3}$] | **n (639 nm)** [±0.001] |
|---|---|---|---|---|---|---|
| **PZG-4N** | 40**P**$_2$O$_5$–55**Z**nO–1**G**a$_2$O$_3$ | **4**Na$_2$O | - | 382 | 3.21 | 1.567 |
| **PZG-2N2A** | 40**P**$_2$O$_5$–55**Z**nO–1**G**a$_2$O$_3$ | **2**Na$_2$O | **2**Ag$_2$O | 385 | 3.30 | 1.570 |

Thermal properties are the main indicator for evaluating the potential of the glasses for optical fiber manufacturing. The $T_g$ of the PZN-4N and PZN-2N2A glasses are $T_g$ = 382 °C and $T_g$ =385 °C respectively. Above all the absence of discernable crystallization events on the Differential Scanning Calorimetry (DSC) scans up to 700 °C attests their suitability for thermal drawing.

Fibers were drawn from a macroscopic scaled-up preform, which is elongated through localized thermal heating while being hold vertically (See *Experimental* section). Phosphate-based preforms are depicted on **Figure 1** ((a) PZG-4N, (b) PZG-4N and PZG-2N2A). It consists of cylindrical macroscopic glass rods of 8 mm in diameter and ~7 cm in length (note: the horizontal base of the preforms, due to the shape of the brass mold, have no influence on the

drawing process). Alternatively rectangular preforms (Figure 1b) were designed, as will be further discussed below. We assessed the drawing ability of both glass compositions. They were brought to their softening temperature regime while temperature, preform-holder motion and capstan velocity were continuously monitored to prevent catastrophic mechanical failure.

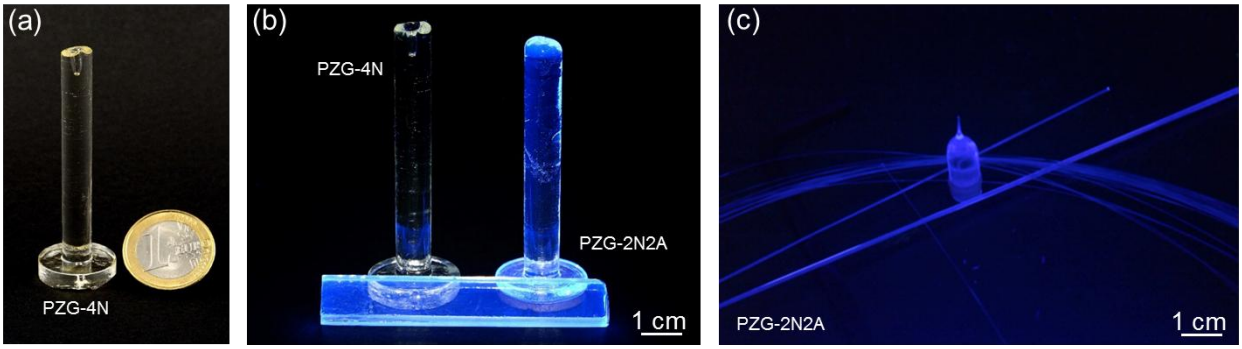



**Figure 1** Phosphate-glass preforms and fibers **(a)** Undoped preform under white light **(b)** Undoped and doped preforms under UV excitation light **(c)** PZG-2N2A glass (bottom-neck preform, capillaries and fiber $l$ ~40 m, $\phi$ ~150 µm) under UV excitation light

Following this procedure, each glass was drawn into ~40-meters-long fibers with diameters ranging $\phi$ = 200 µm, down to 100 µm. Figure 1c depicts a bundle of PZG-2N2A fibers, as well as a bottom-neck preform and two tens-of-centimeter-long capillaries under UV excitation (254 nm). No signs of heterogeneities or inclusions were visually apparent. In order to confirm the optical transparency of the fibers, attenuation measurements were performed by the cut-back method at the wavelengths 1064 and 1550 nm on initial sections of ~1.20 meters.

**Table 2** Fiber loss at $\lambda$ = 1064 nm and $\lambda$ = 1550 nm (measured by the cut-back method)

| Glass | Composition (mol%) | | | 1064 nm [dB.m$^{-1}$] | 1550 nm [dB.m$^{-1}$] |
|---|---|---|---|---|---|
| **PZG-4N** | 40**P**$_2$O$_5$–55**Z**nO–1**G**a$_2$O$_3$ | **4**Na$_2$O | - | 1.8 | 9.7 |
| **PZG-2N2A** | 40**P**$_2$O$_5$–55**Z**nO–1**G**a$_2$O$_3$ | **2**Na$_2$O | **2**Ag$_2$O | 1.6 | 8.5 |

Loss are similar with wavelengths for both compositions (**Table 2**). We find 1.8 dB.m$^{-1}$ and 1.6 dB.m$^{-1}$ at 1064 nm, and 9.7 dB.m$^{-1}$ and 8.5 dB.m$^{-1}$ at 1550 nm for the glasses PZG-4N and PZG-2N2A respectively. We believe the increase in loss observed at 1550 nm relates to the first overtone of the hydroxyl absorption and to the multi-phonons cutting edge of the glass (centered on 3 µm for a sample of 0.5 mm in thickness). Loss measurement proves that the resistance toward devitrification of the selected materials effectively prevents the nucleation and growth of parasitic crystallite centers during the drawing process. Although minimum loss remain relatively high for practical applications, we must note that no purification protocol, other than the use of high-purity precursors, was introduced at this stage. Furthermore measurements were conducted on bare mono-material fiber, with no core/clad geometry or protective polymer cladding involved.

Raman spectroscopy was carried out on the PZG-2N2A bulk, preform and fiber samples in order to assess an eventual structural deviation induced by the drawing process ($\lambda_{Excitation}$ = 532 nm). The three normalized Raman signatures precisely overlap (**Figure 2a**). The Raman spectra are dominated by two broad envelopes centered on 705 and 1175 cm$^{-1}$, assigned respectively to symmetric P-O-P stretching modes and to symmetric stretching of $PO_2^-$ in $P\O_2O_2^-$ tetrahedral units (where Ø is a bridging oxygen) expected for a derived structure of metaphosphate.[20] Less intense peaks at 1000 and 1050 cm$^{-1}$ can be attributed to symmetric and asymmetric stretching

modes of $P\O{O_3}^{2-}$ units forming the end of the phosphate chains.[21, 22] At lower frequencies, the large envelopes peaking at 350 and 550 $cm^{-1}$ are mainly due to bending modes of phosphate units with probably weak contributions coming from gallium and zinc oxides vibrational modes. Similarly, the fluorescence properties of the PZG-2N2A glass before and after drawing have been compared (Figure 2b). Remarkably we observe that the fluorescence emission of the bulk glass is fully preserved in the fiber sample. The PZG-2N2A glass exhibits an excitation band centered on $\lambda$ = 245 nm (due to the absorption band associated with $Ag^+$ ions) and it emits intrinsic fluorescence mainly around $\lambda$ = 368 nm under UV excitation. This emission has been attributed to the $d^{10} \leftrightarrow d^9s^1$ transition of $Ag^+$ ions homogenously dispersed throughout the glassy matrix.[13]

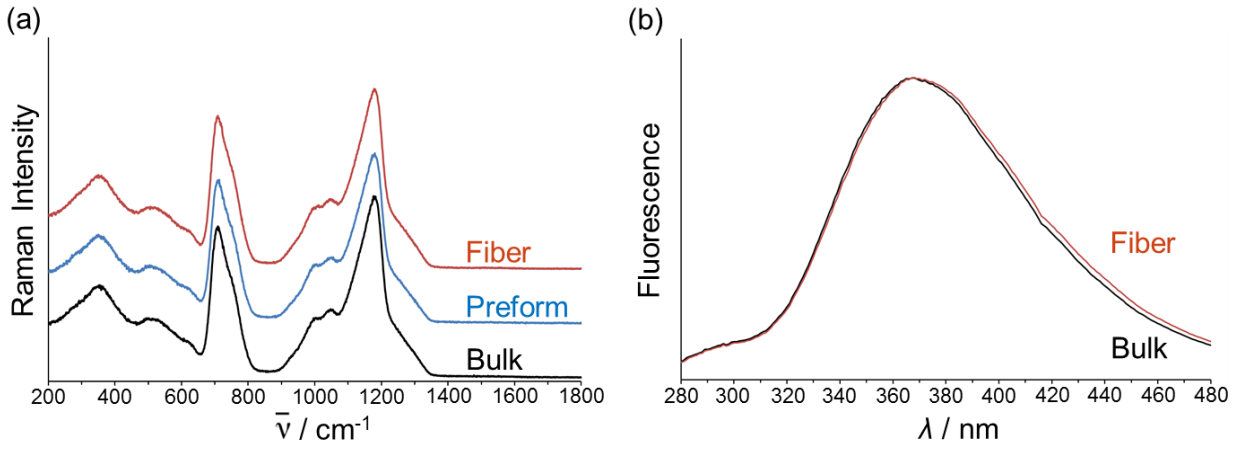



**Figure 2** Silver-doped phosphate glass PZG-2N2A (a) Normalized Raman spectra of the bulk, preform and fiber glass ($\lambda_{Excitation}$ = 532 nm) (b) Normalized fluorescence emission of the bulk versus fiber glass ($\lambda_{Excitation}$ = 245 nm)

The preservation of the luminescence properties of the PZG-2N2A glass is a crucial result as it indicates that neither clustering nor reduction of $Ag^+$ ions species has occurred during the drawing process, although the material is being hold above $T_g$ for approximately one hour. It

ensues from maintaining the material under oxidizing conditions ($O_2$ atmosphere), which prevents the reduction and diffusion of the $Ag^+$ ions.

### 2.2. Silver-containing zinc-phosphate glass ribbon fibers

The thermo-viscous flowing ability of the PZG-2N2A glass, associated with the precise control of the drawing conditions, allows for the fabrication of intrinsically photosensitive phosphate-based fibers. Now we proceed to overtake a more sophisticated and original task, namely the direct preform-to-fiber drawing of a planar, sharp corner-edges device. **Figure 3** outlines our approach to ribbon fiber processing. The procedure starts with the preparation of a macroscopic scale rectangular preform (panel a). For this a glass slab is grinded and optically polished to the proper dimensions (typically: 10-mm wide, 0.4-mm thick, and 80-mm long). The preform is then thermally scaled down into tens-of-meters mechanically flexible flat fiber. Optical and SEM micrographs in panel b depict the longitudinal and cross-sectional views of the fiber (left and right panels respectively) and of its dimensions.

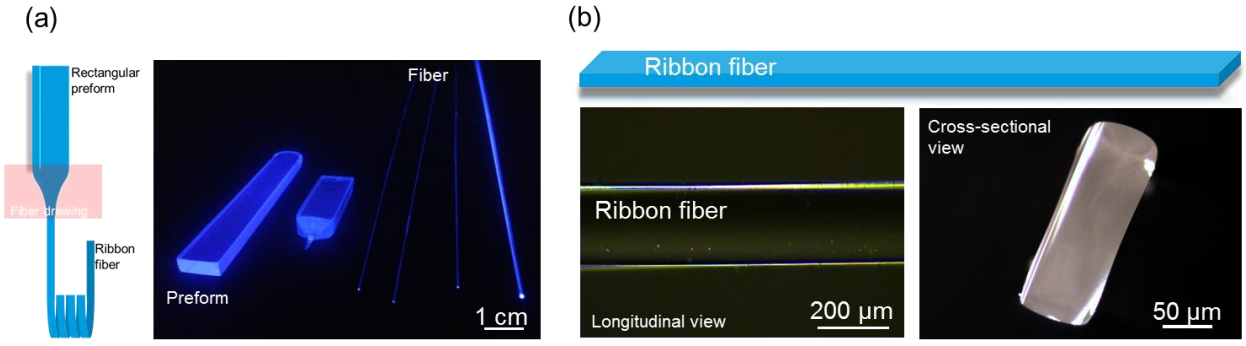



**Figure 3** Thermal drawing of ribbon fibers **(a)** Preform, bottom-neck preform and fiber samples under UV light **(b)** Longitudinal and cross-sectional views (white light)

Ribbon fibers fabrication occurs through homothetic dimensional reduction of the drawn preform. To succeed a stringent viscosity-regime trade-off is imposed to the glass medium during its shaping. Drawing parameters are finely tuned to allow the material to reach its necessary low-viscous fluid state while, in the meantime, it is being maintained in a high-viscosity regime so as to slow down the kinetics of surface energy mechanisms driven during the shaping process. This operation allows preventing transverse features to evolve toward cylindrical shape.

### 2.3. DLW on silver-containing zinc-phosphate glass ribbon fibers

Direct femtosecond laser writing is a powerful method to implement active compounds into zinc phosphate glasses.[14, 15] Herein, taking advantage of the flat, uniform geometry of the ribbon fibers, we generate silver ions clustering in photosensitive PZG-2N2A glass. A ribbon fiber was truncated and exposed to irradiation (**Figure 4a**). DLW was performed typically 50 µm below the surface by linearly moving the fiber sample at controlled speeds along its longitudinal axis (see *Experimental*). Motifs were made of multiple series of lines parallel and perpendicular to the fiber main axis. Laser structuring places stringent requirements on the surface and optical quality of the substrate. Therefore, in this regard, successful DLW carried out in PZG-2N2A fiber first stresses the flatness and homogeneity of the device. Silver ions clustering is triggered by exposing the glass to a high-repetition-rate pulse train from a tightly focused NIR femtosecond laser. It results from multiphoton ionization associated with cumulative thermal effects, allowing for the reduction of $Ag^{+}$ ions, their diffusion and aggregation into $Ag_m^{x+}$ clusters (*m*: number of atoms, $m < 20$; *x*: ionization degree).[23] The clusters are localized at the envelope of the focusing voxel. Under exposure to UV radiations ($\lambda$ = 405 nm), the $Ag_m^{x+}$ clusters emit homogenous fluorescence with a broad spectrum covering the visible range centered on $\lambda$ = 480 nm (Figure 4b).

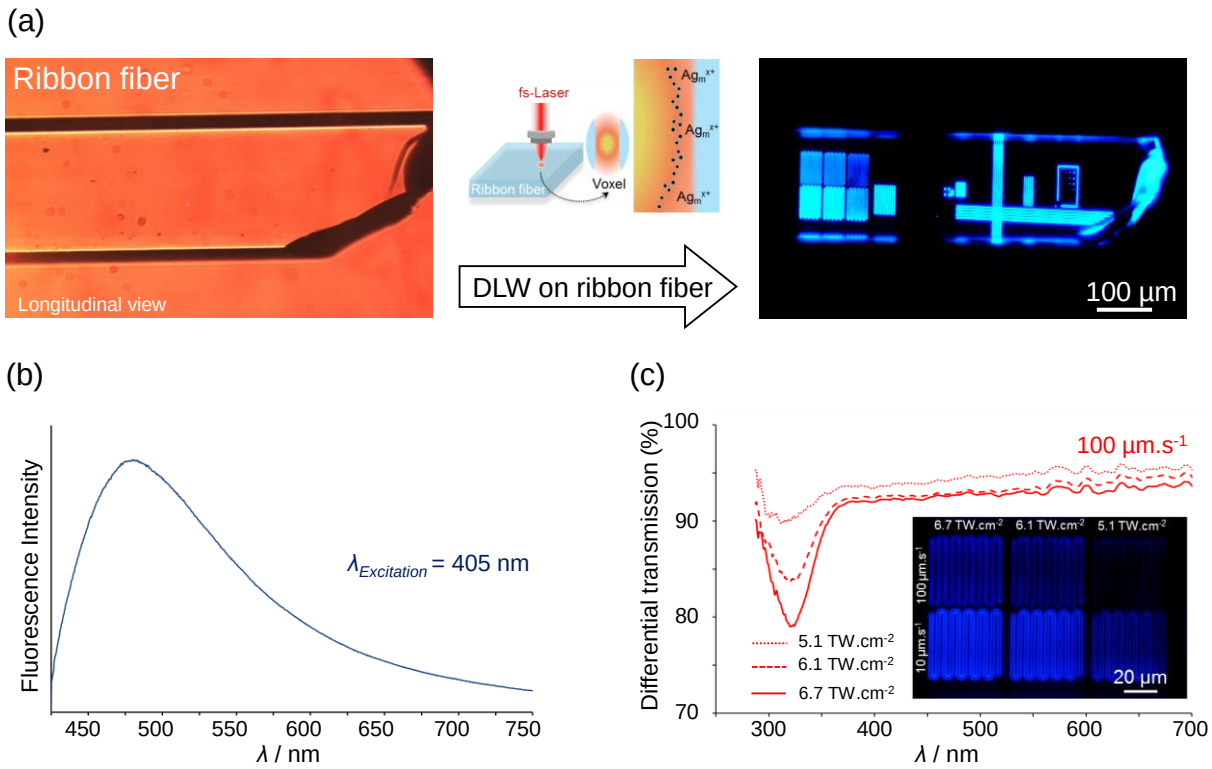



**Figure 4** DLW in ribbon fibers **(a)** Glass PZG-2N2A fiber sample before (under white light) and after irradiation (under UV light, $\lambda_{Excitation}$ = 405 nm) and DLW schematic **(b)** Micro-fluorescence emission spectrum of photo-inscribed $Ag_m^{x+}$ clusters **(c)** Matrix of curvilinear patterns with irradiances and sample motions, and related micro-transmission spectra for $v$ = 100 µm.s$^{-1}$.

In order to highlight the Laser-induced modifications, we have performed differential micro-transmission measurements on structured zones with respect to the pristine glass as a function of the irradiation dose. Six curvilinear patterns were processed for the three irradiance values $I$ = 5.1 TW.cm$^{-2}$, 6.1 TW.cm$^{-2}$ and 6.7 TW.cm$^{-2}$ and for the two sample velocities $v$ = 10 µm.s$^{-1}$ and 100 µm.s$^{-1}$ (corresponding at each position to 2.0 $10^6$ to 2.0 $10^5$ deposited pulses respectively). Figure 4c shows the wide-field fluorescence imaging of the Laser-induced silver clusters. We observe that emitted luminescence, and then that the related concentration of Laser-induced

clusters, increases with the cumulative deposited dose. For clarity we show the differential micro-transmission spectra only for the velocity $v$ = 100 µm.s$^{-1}$. They exhibit an intense absorption band centered at $\lambda$ = 324 nm (E = 3.82 eV) (and a much weaker one around $\lambda$ = 290 nm (E = 4.27 eV)). The amplitude of the multicomponent absorption band around $\lambda$ = 324 nm grows linearly with the deposited dose. These bands have been assigned to $Ag_m^{x+}$ clusters and are in good agreement with previous observations made on the silver zinc-phosphate glass.[23] Finally we note a modification of the baseline of the differential micro-transmission spectra over the whole spectral range, from the ideal 100% value down to 95%, typically. We believe the observed decrease in transmitted light intensity which affects the whole spectral domain is due to scattering effect.

The *in-fiber* Laser-structuring represents an original method for implementing complex light-manipulating architectures. To illustrate its potential we have schematically inscribed optical micro-ring resonators directly in ribbon fibers (**Figure 5a**), without having confirmed and characterized their optical functionalities yet, such demonstration being beyond the scope of this article. The first structure (left-side) consists in a closed resonator ring side-coupled to two light input/output bus waveguides, one of which being addressed from the side of the fiber. Alternatively (right-side) a Mach–Zehnder interferometer made of two arms split from a single source is coupled to one side of the resonator ring. To get confident about the potentiality of this route to generate photonics structures, we aimed at verifying the waveguiding properties of the photo-inscribed $Ag_m^{x+}$ clusters features. To assess such guiding abilities, far field experiments were conducted using a Yb:KGW Laser operating at 1030 nm in CW low-power regime as a light source, hence preventing any glass structuring and multi-photon fluorescence excitation (see *Experimental*). For the purpose of the demonstration, the propagation characteristics were investigated on a bulk sample. This assumption is reasonable since all the here-above described

experiments highlight the fact that both physico-chemical properties and Laser-writing ability are fully preserved from bulk samples to ribbon fibers. A 7-mm-long linear pattern was produced in a silver zinc-phosphate bulk glass (with 4% of molar $Ag_2O$), typically at 100 µm below its surface. Then the sample was rotated 90° in order to allow for Laser injection from above and for the collection of the received guided light from beneath (Figure 5b). Micrograph of the bulk glass and of the fluorescent photo-written tube under broad field UV illumination at 405 nm is depicted on Figure 5c.

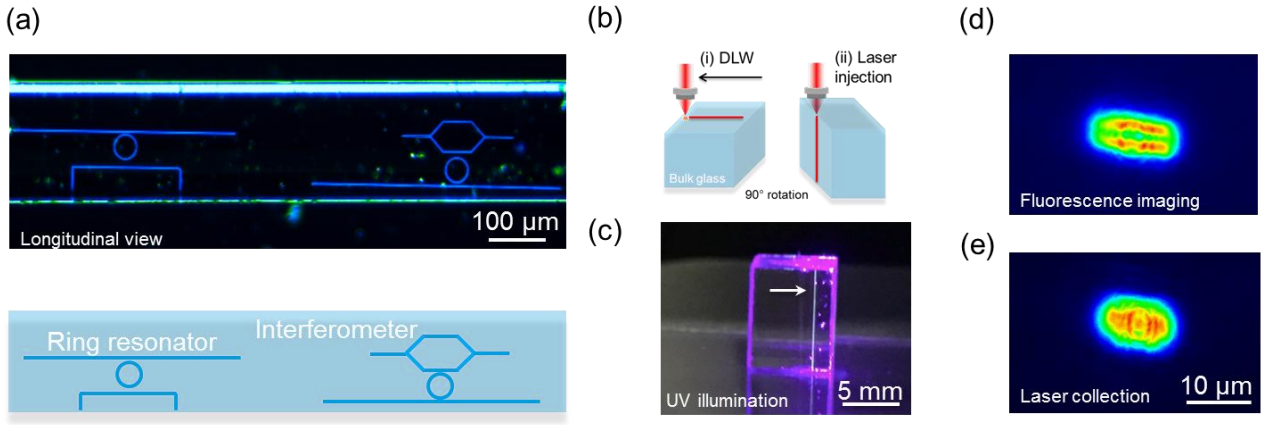



**Figure 5** Waveguiding evidence in silver zinc-phosphate bulk glass **(a)** Ring resonators and Mach-Zehnder interferometer written in ribbon fibers ($\lambda_{Excitation}$ = 405 nm) **(b)** Schematic of the experiment: DLW in the linear x translation followed by 90° rotation of the sample for subsequent Laser injection **(c)** Micrograph of the bulk glass under broad field illumination with 405 nm UV light (arrow: fluorescent photo-written tube) **(d)** Output fluorescence imaging at the bottom plane of the bulk sample upon UV tightly-focused Laser injection at 405 nm **(e)** Injection of the 1030 nm Laser in the written tube and output bottom imaging after its propagation along the 7-mm long guiding structure.

The light from a tightly-focused Laser diode at 405 nm was injected from the top surface of the structured bulk sample while imaging of the induced fluorescence was performed at the bottom plane (Figure 5d). Note that spectral filtering was employed to cancel the incident Laser diode light. The transversal dimensions of the collected spot of photo-luminescent signal from the Laser-written tube are $L \sim 8$ µm and $l \sim 4$ µm. Furthermore it exhibits a double-line shape that is typical of $Ag_m^{x+}$ clusters features.[23] In order to get a clearer demonstration of waveguiding abilities of the structure, the same operation was performed with a tightly-focused CW low-power 1030 nm Laser (Figure 5e), for which no fluorescence is excited. Upon the latter injection, we observe a transmitted Laser light localized on the photo-written features, which demonstrates unambiguously their waveguiding properties. Indeed, since the top injection plane and the bottom imaging plane are 7-mm distant, we claim that the observed light at the bottom imaging plane cannot come from the collection of free propagating injected light. To support the guiding observation we claim, the refractive index variation between the pristine glass and the $Ag_m^{x+}$ clusters areas was estimated using a phase-contrast microscopy method (see *Experimental*), which gives access to the local index modification (providing that the structure thickness had been previously measured by high-resolution confocal microscopy). It showed an increase of the refractive index in the modified region of $\Delta n \sim 5.10^{-3}$ over the visible spectral range, with a spatial distribution corresponding to that of the silver clusters. Further effort is currently engaged to characterize the beam modes, loss and the magnitude of the photo-induced index modification to accurately regulate the propagation of light through the device. Laser-structuring allows for the inscription of perennial silver cluster-based waveguides in fibers, thanks to the thermal and optical stability of the photo-induced clusters.[14, 24] It provides unique opportunities for applications in nonlinear optics, cavity-enhanced spectroscopic sensing, filtering or fully-integrated tunable photonics.

## 3. Conclusion and perspectives

Here we have detailed the methodology for the manufacturing of silver-containing zinc phosphate glass fibers. The fabrication of photosensitive, photo-writable silver-containing phosphate-based ribbon fibers stem from judiciously adjusting both the materials composition and its geometry. We validated in first place the aptitude of the glasses to be shaped into fibers. Loss measurements verify the effective transparency of the fiber in the NIR region. Notably, as evidenced by photo-luminescence measurements, $Ag^{+}$ ions remain homogenously dispersed upon drawing within the glass matrix. The intrinsically photosensitive fibers proposed here authorizes for large amount of silver ions doping without clustering, hence reducing the need for germanium doping or hydrogen-loading. Following we have presented a straightforward manufacturing method of elongated ribbon structures. Cost-limited, photosensitive fibers in a flat format is anticipated to ease the design of high-sensitivity fully-distributed fiber-based dosimeter sensors. Already, silica-based optical flat fibers have been proposed as the basis for such purpose[19] while high irradiation dose studies have been initiated on bulk silver zinc-phosphate glasses.[25] More sophisticated interconnected fiber-based 2D screen may eventually be envisioned for applications in the field of high-dose therapy dosimetry where image reconstruction instruments are needed. The *in-fiber* Laser-structuring scheme enables the integration in a single device of an entire array of unconventional device architectures on a flexible substrate platform. Beyond, we reported recently on structured light-induced DLW of nontrivial fluorescent $Ag_m^{x+}$ topologies obtained using non-Gaussian beam profiles.[26] This result could be exploited for the implementation of innovative photonic architectures relying on the spatial distribution of photo-induced patterns with linear and nonlinear optical properties. Additionally we have shown that, upon subsequent post-irradiation annealing of the glass above $T_g$, $Ag_m^{x+}$ clusters can grow into larger entities, up to metallic nanoparticles.[23] It would allow

for the *in-fiber* sub-micrometric 3D patterning of metal–dielectric composites within low-$T_g$ glass fiber, a promising approach for engineering highly-efficient plasmonic sensing devices or increasingly complex electronic circuits.

Future work will consist in establishing improved glass purification and fiber manufacturing protocols in order to satisfy technological specifications. Other work will consist in developing core-clad fiber structures to propose innovative laser materials and geometry able to handle high flux of photons without premature ageing and, by taking advantage of nonlinear optical processes, to favor all-fiber short-length monolithic systems. Beyond, our approach could lead to a powerful alternative to bottom-up synthesis methods for producing scalable *in-fiber* 3D nano-structured materials, with functionalities spanning sensing, photonics, or even metamaterials devices.

## 4. Experimental Section

*Glasses and preforms synthesis* The zinc-phosphate glasses were melted using the standard melt-quench technique. High-purity precursors (ZnO, $Zn(PO_3)_2$, $Ga_2O_3$, $NaPO_3$, $AgNO_3$) were weighted in powder forms and mixed together in a platinum crucible. The mix was ramped up (1 °C.min$^{-1}$) at 1100 °C and then kept at this temperature for 12 hours. Following the liquid was poured on a brass plate to freeze the melt. Preforms were produced by casting the glass in a specifically designed brass mold, pre-heated at ~ $T_g$-10 °C and annealed at $T_g$-40 °C for 12 hours.

*Fiber drawing* Thermal drawing was performed using a dedicated 3-meters-high optical fiber draw tower composed of an annular electrical furnace with a sharp temperature profile, a diameter monitor, a tension dancer and a collecting drum. The preform was slowly fed into the furnace and the temperature was gradually increased at a rate of 10 °C.mn$^{-1}$ up to ~700 °C under continuous oxygen gas flow (3 l.min$^{-1}$). The preform-holder motion and capstan rotation velocity

were controlled in real-time to produce the targeted fiber diameter. Following this procedure, meters of fibers were drawn with diameters ranging from 250 µm, down to 75 µm.

*Direct Laser Writing* DLW on ribbon fibers was performed with a Yb:KGW femtosecond oscillator (T-Pulse 200, Amplitude Systemes, up to 2.6 W, 9.1 MHz, 390 fs at 1030 nm). The irradiation duration and transmitted irradiance were controlled by an acousto-optic modulator, enabling the accumulation of $N = 10^5$–$10^6$ pulses with energies from 50 to 150 nJ. The positioning and displacement of the sample were performed with a high-precision 3D translation stage (XPS-50 stages, Micro-Contrôle). Irradiations were carried out by focusing laser pulses with a microscope objective (Mitutoyo, APO PLAN NIR, 20×, NA 0.4). In order to highlight waveguiding abilities of the photo-written features, a CW low-power 1.03-µm Laser was injected inside the tube using a microscope objective (Olympus, 20×, NA 0.5). An identical bottom microscope objective was used to collect the transmitted (guided) light, and to conjugate the imaged plane on a CCD camera. With the considered 7-mm long sample, the injection and collection planes of these two objectives were optically distinct, ensuring that any collected light at the bottom plane could only be guided light.

*Characterization instruments* Thermal analysis was performed by differential thermal analysis (DSC 404 PC from Netzsch Inc.). About 20 mg of powdered glass was inserted into a Pt pan and placed in the DSC chamber along with an empty reference pan. Characteristic temperatures were measured as the inflection point of the endotherm at a heating rate of 10 °C/min (precision ±2°C). Refractive indices were measured using Abbe refractometer. Micro-absorption measurements were performed in bright-field using a 'CRAIC Technologies' microscope equipped with a Xenon lamp and a condenser as a white light source. A conjugated 10× magnification microscope objective was used to collect the transmitted light through the laser-induced structures. Raman spectra were recorded with a Xplora Horiba micro-Raman spectrometer using

a 532 nm excitation line with 10 mW of incident power. Raman spectra in the range of 200–2000 $cm^{-1}$ were recorded with a resolution of 2.5 $cm^{-1}$. The macroscopic luminescence spectra (emission and excitation) were recorded at room temperature with a SPEX Fluorolog-2 spectrofluorimeter (Horiba Jobin-Yvon). The excitation source was a 450 W xenon lamp enabling continuous excitation from 200 nm to 800 nm. The signal was detected and amplified by a Hamamatsu R298 photomultiplier. The samples were grounded into powder to cancel geometric effects. Refractive index variation between the pristine glass and the $Ag_m^{x+}$ clusters areas was estimated using a phase-contrast microscopy method with commercially available equipment's from PHASICS Inc.

**Acknowledgements**

The authors wish to thank Frédéric Adamietz for micrographs of the preforms and Arnaud Royon for the helpful discussions. Funding for this work has been provided from the French Government, managed by the French National Research Agency (ANR Grant #40611), by the Programme IdEx at the University of Bordeaux, the Cluster of excellence LAPHIA and by the Aquitaine Region.

Received: ((will be filled in by the editorial staff))

Revised: ((will be filled in by the editorial staff))

Published online: ((will be filled in by the editorial staff))

**REFERENCES**

[1] A. Croteau, A. C. J. Poulin, "Photosensitive Fibers" in *Specialty Optical Fibers Handbook*, Elsevier, London, UK, **2007**.

[2] G. D. Peng, P. L. Chu, "Polymer optical fiber gratings" in *Polymer optical fibers*, American Scientific Publishers, Valencia, CA, **2004**.

[3] M. Bernier, D. Faucher, R. Vallée, A. Saliminia, G. Androz, Y. Sheng, S. L. Chin, *Opt. Lett.* **2007**, *32*, 454.

[4] A. F. Abouraddy, O. Shapira, M. Bayindir, J. Arnold, F. Sorin, D. S. Hinczewski, J. D. Joannopoulos, Y. Fink, *Nat. Mater.*, **2006**, *5*, 532.

[5] A. S. Beddar, *Radiation Measurements*, **2007**, *41*, 124.

[6] B. A. Flusberg, E. D. Cocker, W. Piyawattanametha, J. C. Jung, E. L. M. Cheung, M. J. Schnitzer, *Nat. Methods*, **2005**, *12*, 941.

[7] P. Aiestaran, V. Dominguez, J. Arrue, J. Zubia, *Opt. Mater*., **2009**, *31*, 1101.

[8] S. Pissadakis, A. Ikiades, P. Hua, A. K. Sheridan, J. S. Wilkinson, *Opt. Express* **2004**, *12*, 3131.

[9] S. Suzuki, A. Schülzgen, S. Sabet, J. V. Moloney, N. Peyghambarian, *Appl. Phys. Lett.* **2006**, *89*, 171913.

[10] L. Xiong, P. Hofmann, A. Schülzgen, N. Peyghambarian, J. Albert, *Opt. Mater. Express* **2014**, *4*, 1427.

[11] J. Thomas, E. Wikszak, T. Clausnitzer, U. Fuchs, U. Zeitner, S. Nolte, A. Tünnermann, *Appl. Phys. A* **2007**, *86*, 153.

[12] P. Hofmann, C. Voigtländer, S. Nolte, N. Peyghambarian, A. Schülzgen, *J. Lightwave Technol.* **2013**, *31*, 756.

[13] K. Bourhis, A. Royon, M. Bellec, J. Choi, A. Fargues, M. Treguer, J-J. Videau, D. Talaga, M. Richardson, T. Cardinal, L. Canioni, *J. Non-Cryst. Solids* 356 (2010) 2658.

[14] A. Royon, K. Bourhis, M. Bellec, G. Papon, B. Bousquet, Y. Deshayes, T. Cardinal, L. Canioni, *Adv. Mater.* **2010**, *22*, 5282.

[15] G. Papon, Y. Petit, N. Marquestaut, A. Royon, M. Dussauze, V. Rodriguez, T. Cardinal, L. Canioni, *Opt. Mater. Express* **2013**, *3*, 1855.

[16] D. S. Agafonova, A. I. Sidorov, E. V. Kolobkova, A. I. Ignatiev; N. V. Nikonorov, *Proc. SPIE 9141 Optical Sensing and Detection III* **2014** 91411T.

[17] N. Chocat, G. Lestoquoy, Z. Wang, D. M. Rodgers, J. D. Joannopoulos, Y. Fink, *Adv. Mater.* **2012**, *24*, 5327.

[18] G. Lestoquoy, N. Chocat, Z. Wang, J. D. Joannopoulos, Y. Fink, *Appl. Phys. Lett.* **2013**, *102*, 152908-5.

[19] A. Alawiah, S. Bauk, H. A. Abdul-Rashid, W. Gieszczyk, S. Hashim, G. A. Mahdiraji, N. Tamchek, D. A. Bradley, *Radiat. Phys. Chem.* **2015**, *106*, 73.

[20] L. L. Velli, C. P. E. Varsamis, E. I. Kamitsos, D. Möncke, D. Ehrt, *Phys. Chem. Glasses* **2005**, *46*, 178.

[21] P. Hee, R. Christensen, Y. Ledemi, J. E. C. Wren, M. Dussauze, T. Cardinal, E. Fargin, S. Kroeker, Y. Messaddeq, *J. Mater. Chem. C* **2014**, *2*, 7906.

[22] M. Dussauze, V. Rodriguez, L. Velli, C. P. E. Varsamis, E. I. Kamitsos, *J. Appl. Phys.* **2010**, *107*, 043505.

[23] N. Marquestaut, Y. Petit, A. Royon, P. Mounaix, T. Cardinal, L. Canioni, *Adv. Funct. Mater.* **2014**, *24*, 5824.

[24] A. Royon, K. Bourhis, L. Béchou, T. Cardinal, L. Canioni, Y. Deshayes Microelectronics Reliability **2013**, *53*, 1514.

[25] K. Bourhis, A. Royon, G. Papon, M. Bellec, Y. Petit, L. Canioni, M. Dussauze, V. Rodriguez, L. Binet, D. Caurant, M. Treguer, J-J. Videau, T. Cardinal, *Mater. Res. Bull.* **2013**, *48*, 1637.

[26] K. Mishchik, Y. Petit, E. Brasselet, A. Royon, T. Cardinal, L. Canioni, *Optics Lett.* **2015**, *40*, 201.

**Table of contents entry**

**The thermal drawing of photosensitive silver-containing zinc phosphate glass ribbon fibers is demonstrated.** Structural and luminescence properties of the native glass are preserved. The flat fiber geometry allows for the convenient, accurate Laser inscription of complex luminescent silver clusters patterns within the glass matrix. These fibers offers a promising platform for the design of highly-efficient sensing, photonics or metamaterials devices.

**Keywords**

phosphate, glasses, fiber, photosensitivity, laser inscription

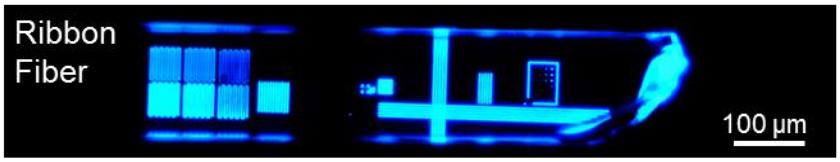
**C. Author 2, D. E. F. Author 3, A. B. Corresponding Author***

F. Désévédavy, Y. Petit, J-C. Desmoulin, A. Abou Khalil, C. Strutynski, M. Dussauze, F. Smektala, T. Cardinal, L. Canioni, S. Danto*

**Title**

Photo-writable Silver-containing Phosphate Glass Ribbon Fibers

**Table of Content figure (55 × 50 mm or 110 × 20 mm)**




Copyright WILEY-VCH Verlag GmbH & Co. KGaA, 69469 Weinheim, Germany, 2013.

**Title**

Photo-writable Silver-containing Phosphate Glass Ribbon Fibers

**Author(s), and Corresponding Author(s)***

*Frédéric Désévédavy, Yannick Petit, Jean-Charles Desmoulin, Alain Abou Khalil, Clément Strutynski, Marc Dussauze, Frédéric Smektala, Thierry Cardinal, Lionel Canioni and Sylvain Danto**